Computational Modeling of a New Fluorescent Biosensor for Caspase Proteolytic Activity Improves Dynamic Range

Jason Jui-Hsuan Chiang* and Kevin Truong, *Member, IEEE*

***Abstract*—The class of fluorescence resonance energy transfer (FRET) protein biosensors that are useful for measuring protease activity is composed of a tandem fusion of yellow fluorescent protein (YFP), a cleavage recognition sequence, and cyan fluorescent protein (CFP). The dynamic range of these FRET-based protein biosensors is often weak, but applications such as high throughput drug screening require stronger dynamic ranges. Using the biosensor for the caspase-3 protease as an example, here we showed a computational approach to improve the FRET dynamic range based on the atomic structure of caspase-3 bound to its inhibitor. This result was verified from our experiments where the FRET dynamic range improved by at least 60% on average in both *in vitro* and *in vivo* contexts. In concept, the same strategy can be applied to improve dynamic range of other FRET-based protein biosensors for protease activity where there exist solved atomic structures for protein complexes.**

***Index Terms*—Biosensor, fluorescence resonance energy transfer (FRET), imaging, protein engineering.**

I. Introduction

RECENTLY, protein biosensors have been created with the ability to observe cellular behavior in single living cells using the phenomenon of fluorescence resonance energy transfer (FRET) between enhanced cyan and yellow fluorescent proteins (ECFP and EYFP, respectively). FRET occurs between a donor fluorophore (such as ECFP) and acceptor fluorophore (such as EYFP), which is dynamically modulated by the relative distance and orientation of the fluorophores [1]. In FRET-based protein biosensors, the change in FRET between ECFP and EYFP is directly correlated with a change in the cellular behavior of interest [1]. Already, FRET-based protein biosensors have been created to measure diverse events such as Ca^{2+} signaling, GTPase activity, protein–protein interaction, and caspase proteolytic cleavage [2]. For instance, a Ca^{2+} biosensor (called cameleon) was created from the tandem protein fusion of ECFP, calmodulin (Ca^{2+} sensing protein), a calmodulin binding domain (CBD), and EYFP [3], [4]. When Ca^{2+} increases, calmodulin binds Ca^{2+} and then binds the CBD, a change that decreases the distance between ECFP and EYFP that increases FRET. When Ca^{2+} decreases, calmodulin releases Ca^{2+} and the CBD that decreases FRET. Therefore, FRET is correlated to Ca^{2+} concentration.

FRET-based protein biosensors generally have weak or low-fidelity signals which can be improved by computational modeling using the solved atomic structure of the protein components. One measure of the strength of the signal is dynamic range, which is defined as the division of the maximum emission ratio (further defined as the division of acceptor emission by donor emission) $R_{\max}$ by the minimum emission ratio $R_{\min}$. Therefore, strategies to improve dynamic range increase $R_{\max}$ or decrease $R_{\min}$. For instance, the $R_{\max}$ of the Ca^{2+} biosensor was improved by computational modeling using the solved atomic structure of calmodulin bound to a different CBD (specifically, calmodulin kinase kinase peptide) which revealed ECFP and EYFP would be theoretically closer in proximity for FRET [4]. Other methods for improving dynamic range involve altering the angle of the fluorophores by random optimization of the linker peptide between ECFP and EYFP [5] and protein fusion of different circularly permutated fluorescent proteins [6].

Computational modeling has not been applied to improving the dynamic range of FRET-based protein biosensors of proteolytic cleavage, such as caspase-3, although numerous solved atomic structures exist. In this paper, we rationally designed a new biosensor with a greater dynamic range to detect caspase cleavage events based on the crystal structure of caspase-3 bound to an irreversible tetrapeptide inhibitor Ac-DVAD-fmk that fits across a narrow cleft on the protease [7]. The caspase-3 protease cleavage of specific sequences within target proteins is a key activating event of an orderly cell death process called apoptosis, whose evasion is associated with tumorigenesis [8]. To observe caspase activation in living cells, numerous groups have successfully constructed biosensors for caspase cleavage [9]–[12] by inserting a recognition sequence between CFP and YFP variants, mostly containing the recognition sequence of caspase-3. Therefore, the activation of the protease results in the loss of FRET. These biosensors allowed, for the first time, biological scientists to image the dynamics of caspase activation in single living cells.

Manuscript received May 11, 2005; revised July 20, 2005. This work was supported in part by the Banting Foundation and in part by the Natural Sciences and Engineering Research Council of Canada (NSERC) under Research Grant RG-PIN 276250. *Asterisk indicates corresponding author.*

*J. J.-H. Chiang is with the Department of Electrical and Computer Engineering (ECE) and Institute of Biomaterials and Biomedical Engineering (IBBME), University of Toronto, Toronto, ON M5S 3G4, Canada (e-mail: jjason.chiang@utoronto.ca).

K. Truong is with Department of Electrical and Computer Engineering (ECE) and Institute of Biomaterials and Biomedical Engineering (IBBME), University of Toronto, Toronto, ON M5S 3G4, Canada (e-mail: kevin.truong@utoronto.ca).

Digital Object Identifier 10.1109/TNB.2005.864020

1536-1241/$20.00 © 2006 IEEE

II. Materials and Methods

A. Computational Modeling

MODELLER [13] version 6.2 was installed on a computer with an Intel Pentium 4 processor and 512 MB of RAM running on a Windows XP operating system. The Protein Data Bank (PDB) files were downloaded describing the atomic structure of yellow fluorescent protein (PDB CODE: 1MYW) [14], cyan fluorescent protein (PDB CODE: 1OXD) [15], and caspase-3 (PDB CODE: 1CP3) [7]. Using MODELLER, nine separate models of biosensors were generated with flexible linkers (ranging in size from 14 to 30 amino acids) containing the DQMD recognition sequence flanked by YFP and CFP. With each of the biosensor models, 30 putative models were generated by MODELLER for a complex between caspase-3 and the biosensor based on the interaction of caspase-3 bound a the DVAD tetrapeptide inhibitor. The DQMD recognition sequence of the FRET biosensor was aligned to the DVAD tetrapeptide inhibitor. Finally, each model was evaluated on a Swiss PDB viewer for unwanted steric hindrances.

B. Constructions of the Plasmids

Using the cassette-based strategy described by Truong *et al.* [16], the plasmid for expressing yDMQDc, pYDMQDctx3, was created by combining four different plasmids: pCfptx3, pYfptx3, pDMQDtx3, and pHistx3. To create pCfptx3 and pYfptx3, the pECFP-1 (Clontech, Mountain View, CA) and pEYFP-1 (Clontech) plasmid, respectively, were amplified with the following primers: forward, 5′-CATGCCATGGGC-CTGACTAGTGTGAGCAAGGGCGAGGAGCTG-3′; reverse, 5′ - CCGCTCGAGTTAGCCGCTAGCGGCGGCGGTCAC-GAACTCCA-3′. The forward primer contained *Nco*I and *Spe*I, sites, while reverse primer contained *Xho*I and *Nhe*I sites. The resulting PCR fragments were digested with *Nco*I-*Xho*I and ligated into the *Nco*I-*Xho*I site of pTriEx-3 (Novagen, Madison, WI) to create pCfptx3 and pYfptx3. To construct pDMQDtx3 and pHistx3, oligonucleotides were flanked by *Nco*I-*Spe*I on the 5′ end and *Spe*I-*Xho*I on the 3′ end that contained the peptide sequences GGASGGASDQMDASGGASGG and GSSHHHHHHSSG in human codon preference, respectively. The oligonucleotides were digested with *Nco*I-*Xho*I and ligated into the *Nco*I-*Xho*I site of pTriEx-3 to create pDMQDtx3 and pHistx3. To create the intermediate pDMQDctx3, pCfptx3 was digested with *Spe*I-*Xho*I and ligated into the *Nhe*I-*Xho*I site of pDMQDtx3. Similarly, to create the intermediate pY-DMQDctx3, pDMQDctx3 was digested with *Spe*I-*Xho*I and ligated into the *Nhe*I-*Xho*I site of pYfptx3. Finally, to create the pHYDMQDctx3, pYDMQDctx3 was digested with *Spe*I-*Xho*I and ligated into the *Nhe*I-*Xho*I site of pHistx3.

C. Protein Purification of Biosensors

E. coli cell strain Rosetta (Novagen) were transformed with the pHYDMQDctx3 plasmid and plated. A single colony was selected and grown overnight in luria broth at 37 °C. Next, the cells were centrifuged and resuspended in the buffer (50 mM Tris-HCl (pH 7.9), 250 mM NaCl, 1% NP-40 and 0.1 mM PMSF). The cells were lysed by sonication and the biosensor was purified using Ni-NTA resin (Qiagen) and eluted from the column in the buffer (10 mM Tris-HCl (pH 7.9), 250 mM NaCl, and 500 mM imidazole). Finally, the sample was dialyzed and concentrated in the buffer (20 mM Hepes (pH 7.5) and 50 mM NaCl).

D. In Vitro Caspase Cleavage Assay and Spectroscopy

All emission spectra were recorded before and after protease treatment using an excitation wavelength of 437 nm at 22 °C using a fluorescence spectrophotometer model RF-5301PC (Shimadzu). The biosensor (1 μM) was diluted in the caspase reaction buffer (20 mM Hepes (pH 7.5), 50 mM NaCl, 0.1% CHAPS, 10 mM EDTA, 5% glycerol, and 10 mM DTT). Two units of various recombinant active caspases (Calbiochem) were incubated with the biosensor at 37 °C for 2 h. To measure the spectra of the completely cleaved biosensor, the biosensor (1 μM) was diluted in the proteinase K reaction buffer (50 mM Tris (pH 7.8) and 10 mM EDTA) and incubated with 0.1 mg/mL of proteinase K at 37 °C for 1 h (Fig. 3).

E. Cell Culture and Transfection

Mouse embryonic fibroblast (MEF) cells were grown at 37 °C with 5% CO_2 in DMEM (Gibco) supplemented with 10% FBS (Gibco). Transfection was performed using Gene-Juice (Novagen).

F. Imaging

A glass-bottom 35-mm culture dish (Maltek) with MEF cells at 30–70% confluency was transfected with the pYDMQDctx3 plasmid (1 μg) expressing the yDMQDc biosensor. Between one to three days afterward, cells were imaged at 22 °C on an Olympus IX70 microscope with a charge-coupled device (CCD) camera (MicroMax 1300YHS) controlled by MetaMorph 4.5r2 software (Universal Imaging). Cells expressing the biosensor were found on the eyepiece by the W-NIBA filter set (Olympus). Dual-emission ratio imaging of biosensors used a 440DF20 excitation for ECFP, a 455DRLP dichotic mirror, and dual emission filters (480DF30 for ECFP, 535DF25 for EYFP) alternated by a Lambda 10-2 filter changer (Sutter Instruments) (Fig. 4). Interference filters were purchased from Omega Optical.

III. Results

A. Computational Modeling

Computational modeling of a FRET-based caspase-3 biosensor using the structure of caspase-3 bound to its inhibitor showed that the optimal linker length for maximal dynamic range is approximately 20 amino acid residues. Dynamic range can be improved by increasing $R_{\max}$ or decreasing $R_{\min}$. $R_{\min}$ is already the minimum as the ECFP and EYFP are completely separated after proteolytic cleavage; however, $R_{\max}$ can be improved by reducing the length of the linker. To estimate the minimal linker size, using the MODELLER [13] software package, we first modeled the atomic structure of a biosensor with a 30 amino acid linker containing a specific four-residue sequence (such as DMQD) [17] that caspase-3 recognizes and then cleaves [Fig. 1(b)]. The last 11 floppy C-terminal residues of the EYFP (the minimal region needed for acquiring fluorescence) were truncated to reduce the effective linker length. The amino acid composition of the linker was mainly glycine for flexibility and serine to deter any hydrophobic effect from

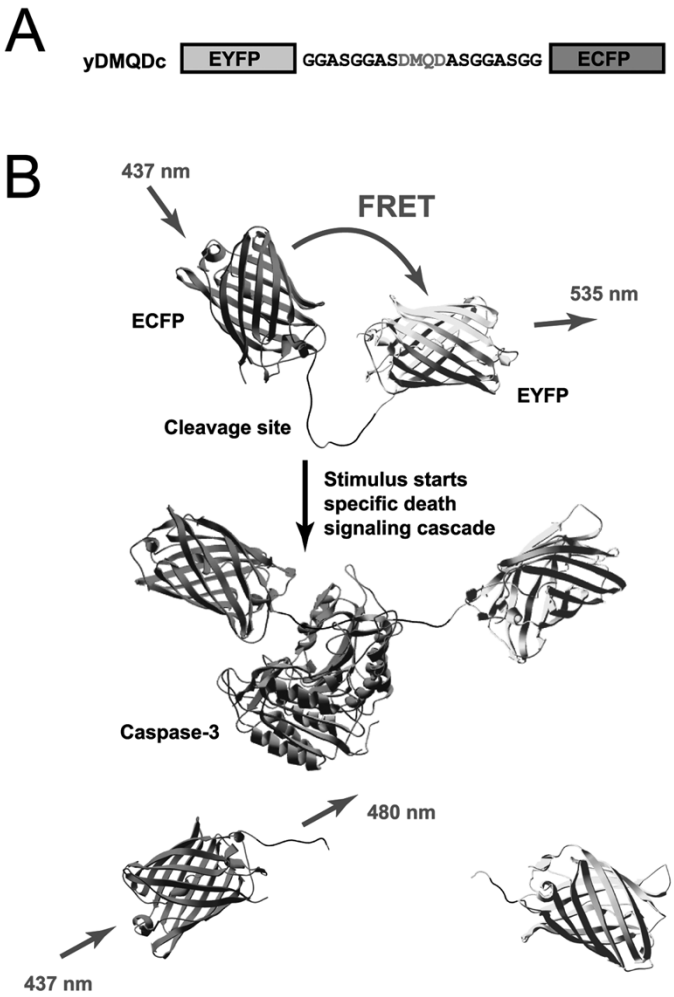

Fig. 1. The design of yDMQDc A, Schematic diagram for yDMQDc. yDMQDc is a tandem fusion of EYFP, a 20-residue linker containing the DMQD recognition sequence, and ECFP. B, A cartoon diagram illustrates the decrease of FRET during the recombinant active Caspase-3 binding. Originally the EYFP is fused with ECFP linked with a 20 residue Caspase-3 specific cut site. The FRET decreases after Caspase-3 cleaves yDMQDc.

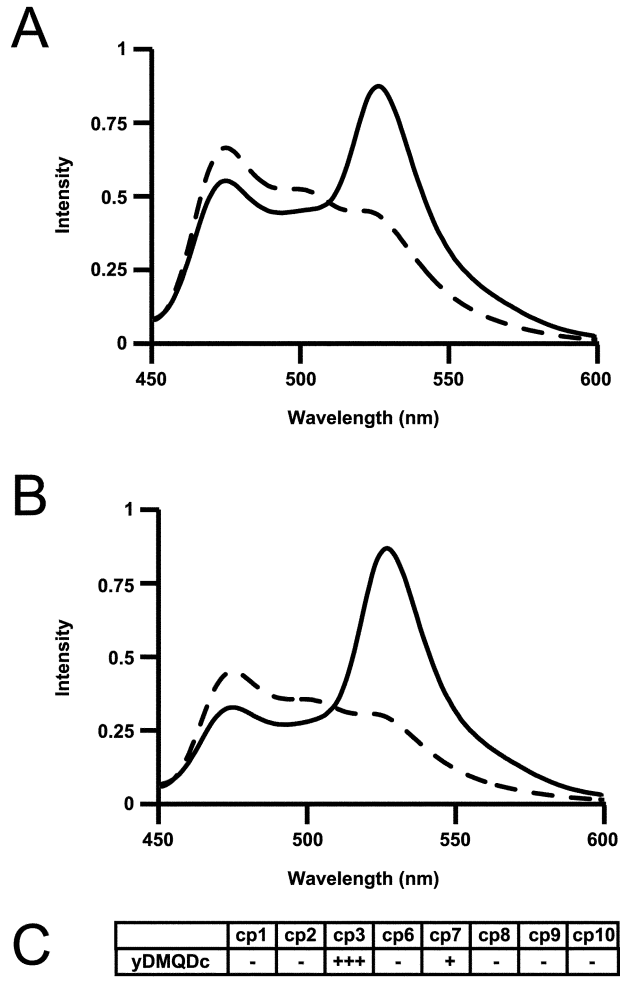

Fig. 2. Fluorescence properties of yDMQDc and C3 *in vitro*. A, B: The emission spectra of yDMQDc and C3 were acquired at an excitation of 437 nm before (solid) and after (dotted) treatment with purified recombinant caspase-3. A: yDMQDc. B: C3. C: Specificity of yDMQDc was determined by estimating the cleavage percentage based on the change in emission ratio after treatment with various caspases ($-$: 0%–5%; $+$: 5%–25%; $++$: 25%–75%; $+ + +$: 75%–100%).

a glycine-rich peptide. Next, the complex of the biosensor was modeled when bound with caspase-3. Then, we iteratively reduced one residue on each end of the linker and applied successive energy optimization functions in MODELLER. When the linker size was reduced to 16 residues, all putative models produced steric clashes between the C-terminal ECFP and caspase-3. Therefore, the optimal length of the linker should be a few residues longer than 16, for instance, 20 [Fig. 1(a)].

B. In Vitro Characterization

Our caspase-3 biosensor (named yDMQDc) showed a greater FRET dynamic range by evaluating the *in vitro* activity against the original caspase-3 biosensor (named C3) from Xu *et al.* [18]. The yDMQDc biosensor consists of a 20 amino acid linker containing the DMQD recognition sequence sandwiched by EYFP and ECFP [Fig. 1(a)]. The DMQD recognition sequence was chosen because it is a highly specific inhibitor to caspase-3. [17] In contrast, the C3 biosensor used a linker of 18 amino acids with the DEVD recognition sequence [18]. However, the actual linker size is 29 residues because they retained the flexible linker from the EYFP. In both the emission spectra of the yDMQDc and C3 biosensor prior to protease treatment, there was a strong peak emission of EYFP (535 nm) due to FRET from ECFP to EYFP [Fig. 2(a), (b)]. Interestingly, the yDMQDc biosensor displayed a larger FRET due to the increase of the emission ratio as shown by an $R_{\max}$ of 2.65 and 1.59 in the yDMQDc and 3C spectra, respectively (Table I). After treatment with recombinant active caspase-3, the peak emission of EYFP decreased and ECFP (480 nm) increased due to an expected loss of FRET [Fig. 2(a), (b)]. When proteinase K was added, the emission spectra did not change showing that caspase-3 efficiently cleaves both yDMQDc and C3. The emission spectra for both yDMQDc and C3 biosensors after caspase-3

TABLE I
SUMMARY OF *IN VITRO* EXPERIMENTAL RESULTS ($n = 5$ EXPERIMENTS)

Biosensor	R_{max}	R_{min}	Dynamic range
C3	1.59 ± 0.01	0.69 ± 0.01	2.30 ± 0.03
yDMQDc	2.65 ± 0.03	0.71 ± 0.005	3.73 ± 0.04

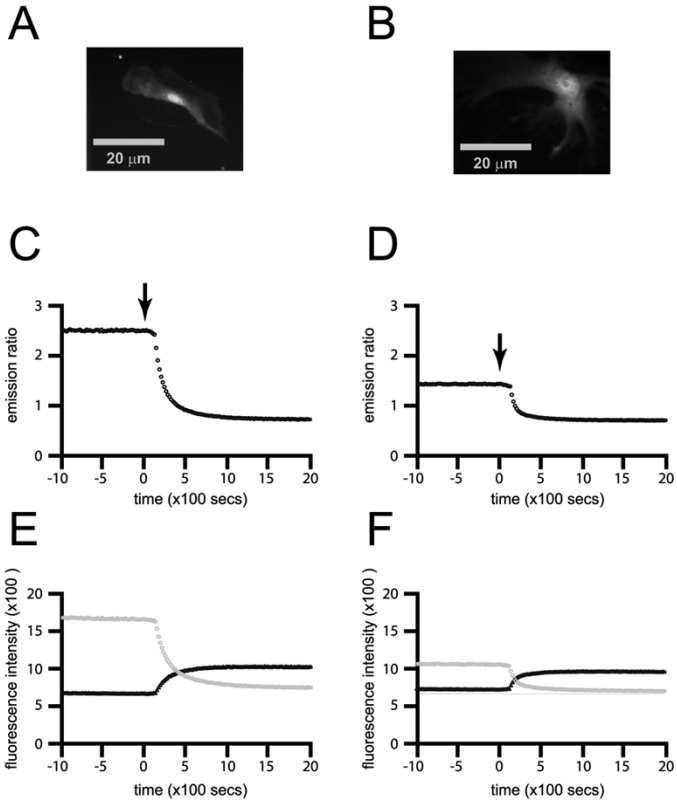

Fig. 3. Imaging temporal events of MEF cells transfected with yDMQDc and C3 indicator. A, B: The fluorescence image (440 ± 10 nm excitation, 535 ± 12.5 nm emission) of MEF cells transfected with yDMQDc and C3 indicator, respectively. C, D: The MEF cells were stimulated with 10 μM staurosporine. E, F: The emission ratios (from 535 ± 12.5 nm to 480 ± 12.5 nm) and intensities (535 ± 12.5 nm and 480 ± 12.5 nm) of the cells were measured every 5 s by digital imaging microscopy. The arrow indicates the estimated time that caspase-3 cleavage occurs.

cleavage were similar with an $R_{\min}$ of 0.71 and 0.69, respectively. This finding was expected because the relative distance and orientation of completely separated ECFP and EYFP at a 1:1 ratio should be the same and therefore the emission spectra is the same. Therefore, as the dynamic range $(R_{\max}/R_{\min})$ of yDMQDc and C3 was 3.73 and 2.30, respectively, it improved by 62% on this sample set. Further studies showed that the dynamic range was improved 61% on average ($n = 5$ experiments). Lastly, our studies further showed that the yDMQDc biosensor is cleaved specifically by caspase-3 [Fig. 2(c)].

C. Live Cell In Vivo Imaging

The yDMQDc biosensor design displayed greater *in vivo* dynamic range over the C3 biosensor by imaging the FRET change in transfected mouse embryonic fibroblast (MEF) cells. In the MEF cells expressing yDMQDc and C3, the fluorescence from the biosensors was distributed in the cytoplasm and the nucleus [Fig. 3(a), (b)]. To induce apoptosis, a $[10\ \mu\text{M}]_f$ staurosporine (STS) stimulus was used. STS is a broad spectrum protein kinase inhibitor that induces apoptosis in fibroblast cells through pathways that ultimately activate caspase-3 [19]. The time course of the spatially-averaged emission fluorescence intensities and ratios was measured in single MEF cells [Fig. 3(c), (d)]. Prior to the STS treatment, the EYFP/ECFP emission ratio, $R_{\max}$, for yDMQDc and C3 was 2.44 and 1.38, respectively

TABLE II
SUMMARY OF *IN VIVO* EXPERIMENTAL RESULTS ($n = 9$ EXPERIMENTS)

Biosensor	R_{max}	R_{min}	Dynamic range
C3	1.38 ± 0.03	0.85 ± 0.03	1.62 ± 0.07
yDMQDc	2.44 ± 0.08	0.88 ± 0.02	2.77 ± 0.11

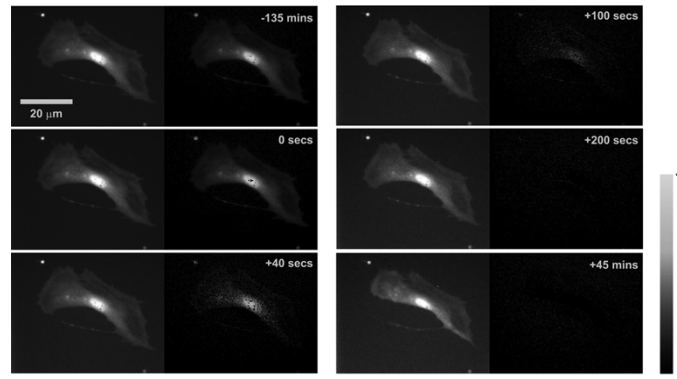

Fig. 4. Imaging spatial events of an MEF cell transfected with yDMQDc. The 10μM STS stimulus was added at −135 min. Time 0 s indicates the estimated time for when caspase-3 activation begins. The left subpanel is the fluorescence image (440 ± 10 nm excitation, 480 ± 12.5 nm emission); the right subpanel is the ratiometric image, where the ratio ranges from $R_{\max}$ (gray) to $R_{\min}$ (black).

(Table II). After treatment, the emission ratio of both FRET biosensors remained constant for about 2 h. Then, there was a decrease in the EYFP emission intensity and an increase in the ECFP emission intensity as expected by the loss of FRET by caspase-3 induced cleavage of the biosensors. Correspondingly, the emission ratio dropped. After the completion of caspase-3 activation, the $R_{\min}$ for yDMQDc and C3 was 0.88 and 0.85, respectively. Therefore, as the dynamic range $(R_{\max}/R_{\min})$ of yDMQDc and C3 was 2.77 and 1.62, respectively, it improved by 71% on this sample set. Further studies showed that the dynamic range was improved 64% on average ($n = 9$ experiments).

D. Morphology Changes

In addition to kinetic information on caspase-3 cleavage, yDMQDc biosensor allowed us to correlate timing of caspase-3 activation with spatial events such as morphology change in apoptosis. In particular, during apoptosis, cells gradually shrink and become round or circular because the cytoskeletal proteins are cleaved by activated caspases inside the cell. When caspase-3 activation started, it occurred evenly throughout the cell as shown by the uniform decrease of the emission ratio (Fig. 4). Furthermore, the majority of the yDMQDc biosensor was cleaved within 5 min and then cell shrinkage gradually occurred. Therefore, morphology change is a downstream event of caspase-3 activation.

IV. DISCUSSION

By employing computational modeling on solved atomic structures, we have designed a new FRET-based protein biosensor for detecting caspase-3 activation that displayed an increase in dynamic range both *in vitro* and *in vivo*. Computational modeling showed that the linker length of the biosensor for maximal dynamic range is approximately 20 residues. To verify the modeling results, the yDMQDc biosensor was

created and compared against the C3 biosensor. There was variability in the actual $R_{\max}$ and $R_{\min}$ values obtained between the *in vitro* and *in vivo* experiments resulting from the differences in optical properties caused by the instrumentation and/or cellular context. However, the relative improvement in dynamic range was consistent from both *in vitro* and *in vivo* experiments at 61% and 64%, respectively. While the FRET dynamic range was improved, it could have resulted from an optimized orientation or distance between the donor and acceptor fluorophores. In the cleaved form of both yDMQDc and C3 biosensors, the relative orientation and distance of the fluorophores is the same. In the uncleaved form, the orientation factor is also the same as the fluorophores have free rotation along the flexible linker, whereas, in contrast, the distance factor is decreased in the yDMQDc biosensor as the linker is shorter. Thus, the improved dynamic range was determined by the distance factor optimized by our computational modeling.

V. Conclusion

Using a computational modeling approach to optimize the distance factor of FRET, a caspase-3 proteolytic biosensor was created that showed an improved dynamic range. In experiments that require a strong signal, this enhancement will have an immediate impact. For example, this biosensor would benefit the high-throughput drug screening of compounds that induce caspase-dependent apoptosis because weak signals are emitted from small cell densities. Furthermore, this biosensor could be incorporated into the genome of a model organism (such as *C. elegans*, *D. melanogaster*, and *X. laevis*) for imaging caspase-3 activity throughout the development cycle, where there is strong interference from autofluorescence. Lastly, the computational approach for biosensor design presented in this work has a long term impact to the imaging of other proteases that have been identified as important prognostic indicators of diseases such as HIV-1 protease, kallikreins, metalloproteases, and cathepsins.

References

[1] K. Truong and M. Ikura, "The use of FRET imaging microscopy to detect protein–protein interactions and protein conformational changes *in vivo*," *Curr. Opin. Struct. Biol.*, vol. 11, pp. 573–578, 2001.

[2] J. Zhang, R. E. Campbell, A. Y. Ting, and R. Y. Tsien, "Creating new fluorescent probes for cell biology," *Nature Rev. Mol. Cell Biol.*, vol. 3, pp. 906–918, 2002.

[3] A. Miyawaki, J. Llopis, R. Heim, J. M. McCaffery, J. A. Adams, M. Ikura, and R. Y. Tsien, "Fluorescent indicators for Ca2+ based on green fluorescent proteins and calmodulin," *Nature*, vol. 388, pp. 882–887, 1997.

[4] K. Truong, A. Sawano, H. Mizuno, H. Hama, K. I. Tong, T. K. Mal, A. Miyawaki, and M. Ikura, "FRET-based *in vivo* Ca2+ imaging by a new calmodulin-GFP fusion molecule," *Nature Struct. Biol.*, vol. 8, pp. 1069–1073, 2001.

[5] T. Nagai and A. Miyawaki, "A high-throughput method for development of FRET-based indicators for proteolysis," *Biochem. Biophys. Res. Commun.*, vol. 319, pp. 72–77, 2004.

[6] T. Nagai, S. Yamada, T. Tominaga, M. Ichikawa, and A. Miyawaki, "Expanded dynamic range of fluorescent indicators for Ca(2+) by circularly permuted yellow fluorescent proteins," *Proc. Nat. Acad. Sci. USA*, vol. 101, pp. 10 554–1059, 2004.

[7] P. R. Mittl, S. Di Marco, J. F. Krebs, X. Bai, D. S. Karanewsky, J. P. Priestle, K. J. Tomaselli, and M. G. Grutter, "Structure of recombinant human CPP32 in complex with the tetrapeptide acetyl-Asp-Val-Ala-Asp fluoromethyl ketone," *J. Biol. Chem.*, vol. 272, pp. 6539–6547, 1997.

[8] D. Kanduc, A. Mittelman, R. Serpico, E. Sinigaglia, A. A. Sinha, C. Natale, R. Santacroce, M. G. Di Corcia, A. Lucchese, L. Dini, P. Pani, S. Santacroce, S. Simone, R. Bucci, and E. Farber, "Cell death: Apoptosis versus necrosis (review)," *Int. J. Oncol.*, vol. 21, pp. 165–170, 2002.

[9] L. Tyas, V. A. Brophy, A. Pope, A. J. Rivett, and J. M. Tavare, "Rapid caspase-3 activation during apoptosis revealed using fluorescence- resonance energy transfer," *EMBO Rep.*, vol. 1, pp. 266–270, 2000.

[10] K. Q. Luo, V. C. Yu, Y. Pu, and D. C. Chang, "Application of the fluorescence resonance energy transfer method for studying the dynamics of caspase-3 activation during uv-induced apoptosis in living hela cells," *Biochem. Biophys. Res. Commun.*, vol. 283, pp. 1054–1060, 2001.

[11] M. Rehm, H. Dussmann, R. U. Janicke, J. M. Tavare, D. Kogel, and J. H. Prehn, "Single-cell fluorescence resonance energy transfer analysis demonstrates that caspase activation during apoptosis is a rapid process. Role of caspase-3," *J. Biol. Chem.*, vol. 277, pp. 24 506–24 514, 2002.

[12] K. Takemoto, T. Nagai, A. Miyawaki, and M. Miura, "Spatio-temporal activation of caspase revealed by indicator that is insensitive to environmental effects," *J. Cell Biol.*, vol. 160, pp. 235–243, 2003.

[13] A. Fiser and A. Sali, "Modeller: Generation and refinement of homology-based protein structure models," *Methods. Enzymol.*, vol. 374, pp. 461–491, 2003.

[14] A. Rekas, J. R. Alattia, T. Nagai, A. Miyawaki, and M. Ikura, "Crystal structure of venus, a yellow fluorescent protein with improved maturation and reduced environmental sensitivity," *J. Biol. Chem.*, vol. 277, pp. 50 573–50 578, 2002.

[15] J. H. Bae, M. Rubini, G. Jung, G. Wiegand, M. H. Seifert, M. K. Azim, J. S. Kim, A. Zumbusch, T. A. Holak, L. Moroder, R. Huber, and N. Budisa, "Expansion of the genetic code enables design of a novel "gold" class of green fluorescent proteins," *J. Mol. Biol.*, vol. 328, pp. 1071–1081, 2003.

[16] K. Truong, A. Khorchid, and M. Ikura, "A fluorescent cassette-based strategy for engineering multiple domain fusion proteins," *BMC Biotechnol.*, vol. 3, pp. 1–8, 2003.

[17] H. Hirata, A. Takahashi, S. Kobayashi, S. Yonehara, H. Sawai, T. Okazaki, K. Yamamoto, and M. Sasada, "Caspases are activated in a branched protease cascade and control distinct downstream processes in Fas-induced apoptosis," *J. Exp. Med.*, vol. 187, pp. 587–600, 1998.

[18] X. Xu, A. L. Gerard, B. C. Huang, D. C. Anderson, D. G. Payan, and Y. Luo, "Detection of programmed cell death using fluorescence energy transfer," *Nucleic Acids Res.*, vol. 26, pp. 2034–2035, 1998.

[19] A. C. Johansson, H. Steen, K. Ollinger, and K. Roberg, "Cathepsin D mediates cytochrome c release and caspase activation in human fibroblast apoptosis induced by staurosporine," *Cell Death Differ.*, vol. 10, pp. 1253–1259, 2003.

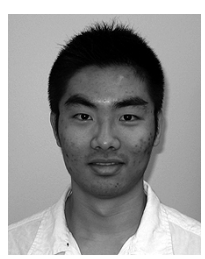

Jason Jui-Hsuan Chiang received the B.A.Sc degree from the Department of Engineering Physics, University of British Columbia, Vancouver, BC, Canada, in 2004. He is currently working toward the M.A.Sc degree in the Department of Electrical and Computer Engineering in collaboration with Institute of Biomaterials and Biomedical Engineering at the University of Toronto, Toronto, ON, Canada.

His previous area of research involved protein engineering. He is now working on improving bioinformatics algorithm with FPGA computing systems.

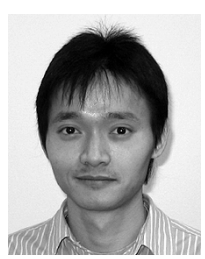

Kevin Truong (M'05) received the B.A.Sc degree in computer engineering and the Ph.D degree in medical biophysics from the University of Toronto, Toronto, ON, Canada, in 1999 and 2003, respectively.

He is currently an Assistant Professor in the Department of Electrical and Computer Engineering and the Institute of Biomaterials and Biomedical Engineering at the University of Toronto. He is a member of the editorial board for *Biotechnology Letters*. His research interests are in the development of bioinformatic algorithms and protein engineering of fluorescent biosensors.

Dr. Truong is a member of the organizing committee for the 28th Annual International Conference of the IEEE Engineering in Medicine and Biology.